Water Research 178 (2020) 115799

Contents lists available at ScienceDirect

Water Research

journal homepage: www.elsevier.com/locate/watres

A knowledge discovery framework to predict the N_2O emissions in the wastewater sector

V. Vasilaki [a], V. Conca [b], N. Frison [b], A.L. Eusebi [c], F. Fatone [c], E. Katsou [a, *]

[a] Department of Civil & Environmental Engineering, Brunel University London, Uxbridge, UB8 3PH, UK
[b] Department of Biotechnology, University of Verona, Strada Le Grazie 15, 37134, Verona, Italy
[c] Department SIMAU, Faculty of Engineering, Polytechnic University of Marche, Via Brecce Bianche 12, Ancona, Italy

ARTICLE INFO

Article history:
Received 17 December 2019
Received in revised form
4 March 2020
Accepted 3 April 2020
Available online 10 April 2020

Keywords:
Short-cut enhanced nutrients abatement - SCENA
Long-term dissolved N_2O and Energy consumption monitoring, knowledge discovery and data mining

ABSTRACT

Data Analytics is being deployed to predict the dissolved nitrous oxide (N_2O) concentration in a full-scale sidestream sequence batch reactor (SBR) treating the anaerobic supernatant. On average, the N_2O emissions are equal to 7.6% of the NH_4–N load and can contribute up to 97% to the operational carbon footprint of the studied nitritation-denitritation and via-nitrite enhanced biological phosphorus removal process (SCENA). The analysis showed that average aerobic dissolved N_2O concentration could significantly vary under similar influent loads, dissolved oxygen (DO), pH and removal efficiencies. A combination of density-based clustering, support vector machine (SVM), and support vector regression (SVR) models were deployed to estimate the dissolved N_2O concentration and behaviour in the different phases of the SBR system.

The results of the study reveal that the aerobic dissolved N_2O concentration is correlated with the drop of average aerobic conductivity rate (spearman correlation coefficient equal to 0.7), the DO (spearman correlation coefficient equal to −0.7) and the changes of conductivity between sequential cycles. Additionally, operational conditions resulting in low aerobic N_2O accumulation (<0.6 mg/L) were identified; step-feeding, control of initial NH_4^+ concentrations and aeration duration can mitigate the N_2O peaks observed in the system. The N_2O emissions during aeration shows correlation with the stripping of accumulated N_2O from the previous anoxic cycle. The analysis shows that N_2O is always consumed after the depletion of NO_2^- during denitritation (after the "nitrite knee"). Based on these findings SVM classifiers were constructed to predict whether dissolved N_2O will be consumed during the anoxic and anaerobic phases and SVR models were trained to predict the N_2O concentration at the end of the anaerobic phase and the average dissolved N_2O concentration during aeration. The proposed approach accurately predicts the N_2O emissions as a latent parameter from other low-cost sensors that are traditionally deployed in biological batch processes.

1. Introduction

In recent years the sustainability and operational efficiency of wastewater treatment plants (WWTPs) have come to the fore (Liu et al., 2018). Several biological technologies such as partial-nitritation − anammox (anaerobic ammonium oxidation) have emerged, towards the efficient, low-cost treatment of high-strength municipal wastewater streams (Lackner et al., 2014; Zhou et al., 2018). The anaerobic supernatant is a by-product of dewatering of the anaerobic digestion effluent and represents less than 1–2% of the total influent flow in the WWTP. It contains 10–30% of the N load and 20–30% of the P load (Janus and van der Roest, 1997; van Loosdrecht and Salem, 2006). Sidestream treatment of the anaerobic supernatant can contribute to the reduction of energy consumption for N-removal, decrease of nitrogen loads in the secondary treatment, and the minimisation of risks related to exceeding effluent regulatory requirements of nitrogen concentrations in the water line of WWTPs (Eskicioglu et al., 2018). However, the performance and environmental evaluation of different sidestream technologies is still under investigation (Eskicioglu et al., 2018; Rodriguez-Garcia et al., 2014).

SCENA (Short-Cut Enhanced Nutrient Abatement) is a new sidestream process, that combines the conversion of NH_4^+ to NO_2^-

* Corresponding author.
E-mail address: evina.katsou@brunel.ac.uk (E. Katsou).

https://doi.org/10.1016/j.watres.2020.115799

under aerobic conditions (nitritation) with the subsequent reduction of NO_2^- to nitrogen gas and enhanced biological phosphorus uptake by polyphosphate-accumulating organisms (DPAOs) in a sequencing batch reactor (SBR) (Frison et al., 2015). External volatile fatty acids (VFAs), are produced via acidogenic fermentation of the primary and secondary sludge on-site and dosed into the SBR. In a recent study, Longo et al. (2016), quantified the environmental and cost benefits and impacts of the integration of the SCENA process in a full-scale WWTP. They reported major energy savings for aeration after the integration of sidestream SCENA process. The direct N_2O emissions were equal to 1.42% of the influent N-load. Short-term monitoring campaigns were implemented, while the effect of operational conditions on N_2O generation was not investigated.

N_2O is a potent cause of global warming, its global warming potential is 265–298 times more than that of CO_2 (IPCC, 2013). The emission of N_2O in full-scale sidestream partial-nitritation/partial-nitritation–anammox or nitrification-denitrification systems range from 0.17% to 5.1% of the influent N-load (average equal to ~2.1% of the N-load is emitted (Vasilaki et al., 2019). Schaubroeck et al. (2015) showed that N_2O emissions from a full-scale sidestream DEMON process in Austria were significantly higher than the direct N_2O emissions from the mainstream treatment in a full-scale WWTP. On average, 0.256 g N_2O were emitted compared to 0.005 g emitted in the secondary treatment per m^3 treated wastewater. The increased direct N_2O emissions can be mainly attributed to low DO concentrations, higher ammonia oxidation rates (AOR) and NO_2^- build-up (Desloover et al., 2011; Kampschreur et al., 2008); conditions that also prevail in the SCENA process. The variability of EF reported in sidestream technologies can be partially attributed to both complex relationships between emitted N_2O and operational conditions and different configurations (i.e. SBR, continuous systems), loads (i.e. NH_4^+ concentrations), feeding strategies and operational control (i.e. DO set-points). Additionally, different interactions between operational variables trigger a different response of N_2O generation. For instance, in a recent modelling study of a granular one-stage partial-nitritation-anammox reactor, Wan et al. (2019) showed that higher temperatures resulted in increased N_2O emissions in the presence of COD (chemical oxygen demand) and in decreased N_2O emissions in the absence of COD (due to increased anammox activity and reduction of NO_2^- accumulation in higher temperature). Additionally, the long-term temporal variations of direct N_2O emissions were not adequately assessed in sidestream technologies; the majority of the monitoring campaigns in sidestream reactors lasted less than 5 days (Vasilaki et al., 2019).

The digitalisation of water services and the data-driven knowledge discovery from wastewater treatment plant may increase the resilience of water utilities under climate change and other water-related challenges (Sarni et al., 2019). Recent studies have provided extensive overviews of the use of data-driven techniques in the wastewater sector for different applications including the development of soft-sensors, fault prediction and multi-objective optimisation of control of water utilities (Corominas et al., 2018; Haimi et al., 2013; Newhart et al., 2019). Data-mining and extraction of the information hidden in the raw sensor signals can facilitate the identification of patterns and hidden structures and reveal significant information on the behaviour of N_2O emissions in continuous wastewater treatment processes (Vasilaki et al., 2018). The SBR in the SCENA process is multiphase (i.e. anaerobic, aerobic, anoxic conditions) applying different operational variables (unsynchronised data), non-linear and subject to different disturbances, such as influent compositions and fermentation liquid characteristics. Moreover, SBR process data are based on a 3d-structure that consists of the number of i) cycles, ii) variables and iii) sampling points within each cycle. Therefore, the identification of process abnormalities and patterns can be complicated. N_2O emissions could be affected by both within-cycle and between-cycle batch dynamics.

In this study, sensor and laboratory analyses data from a full-scale SCENA SBR were analysed to provide insights on the N_2O emissions behaviour and generation. A structured approach was followed for knowledge discovery from the available dataset using a combination of abnormal events detection, classification and regression techniques. The objectives of the study were to i) investigate whether the sensors integrated in the system (i.e. conductivity, pH) can provide actionable information on the dynamics of N_2O emissions, ii) detect hotspots for the accumulation and emission of N_2O and iii) develop data-driven regression and classification models to predict the dissolved N_2O behaviour and concentration for the different phases (anaerobic, aerobic, anoxic) of the SBR.

2. Materials and methods

2.1. Process description and data origin

The Carbonera plant is designed to treat domestic wastewater of a population equivalent of 40,000 (dry weather flow equal to 10,000 m^3/d). After screening and degritting and primary sedimentation, the effluent from the primary clarifier is sent to a Schreiber reactor (single basin – working volume 4671 m^3). Schreiber reactor effluent is pumped to two secondary clarifiers (2260 m^3 each) and subsequently to the tertiary treatment unit for disinfection and filtration before final discharge in the Melma River.

Waste activated sludge (WAS) generated by the biological treatment is recycled to the primary sedimentation unit and mixed with primary sludge. The final concentration of the thickened mixed sludge is around 5% total solids (TS). About 75% of the mixed thickened sludge is fed to an anaerobic digestion unit (1800 m^3 working volume). Digestate is dewatered by a centrifuge with the addition of polyelectrolyte; the solid fraction is mechanically composted and used as agricultural fertilizer. The anaerobic supernatant is sent to the equalization tank (of 90 m^3) in the SCENA system for the biological N and P removal.

The remaining portion of mixed sludge (25%) is fed to a sequencing batch fermentation reactor (SBFR) with hydraulic retention time (HRT) equal to 5 days. The SBFR is operated under mesophilic condition (37 °C) for the fermentation of thickened sewage sludge and the on-site production of carbon source enriched of VFAs (mainly acetic and propionic acids). Daily, around 10 m^3 of fermentation sludge are extracted and replaced with fresh thickened sludge. The solid/liquid separation of the fermented sewage sludge is carried out by a screw-press (SCAE), generating ~2–4 m^3/h of fermentation liquid rich of VFAs (in total, ~110.5 m^3/d). The latter is collected in a storage tank of 20 m^3 and automatically dosed during the anaerobic and anoxic phases of a short-cut sequencing batch reactor (SBR) based on pH and conductivity sensors. The solid fermented fraction (13–15% TS based) is mixed with the thickened mixed sludge and fed to the anaerobic digestor.

The anaerobic supernatant is treated in an SBR with a maximal working volume of 70 m^3 (3–4 cycles daily). The SBR is fed with ~7–9 m^3 of anaerobic supernatant in each cycle that is treated via nitrite enhanced phosphorus removal associated with nitritation-denitritation (SCENA process). The typical SBR (Fig. 1) cycle consists of feeding (6–8 min), anaerobic conditions (30 min), aerobic conditions (200–240 min), anoxic (~60–140 min), settling (30 min) and discharge (8 min). The sensors integrated in the SBR include: pH, Dissolved Oxygen (DO), conductivity, Oxidation Reduction Potential (ORP), mixed liquor suspended Solids (MLSS) and

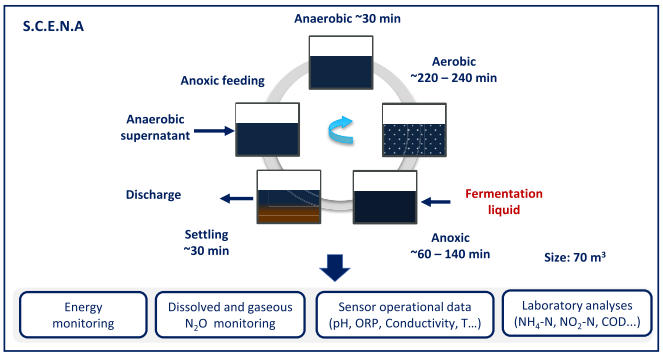

Fig. 1. Schematic representation of a complete cycle in the S.C.E.N.A process and datasets used in the analysis.

temperature. Conductivity and pH are used to control the length of the aerobic and anoxic phases and the carbon source dosage. Additionally, variable frequency driver is used to control the air flow-rate of the blowers, maintaining the dissolved oxygen during aerobic phase in the range of 1.0–1.5 mg/L. The aeration system consists of volumetric blowers (nominal power 11 kW) and n80 diffusers (INVENT), providing ~500 m^3/h of compressed air at 400 mbar of pressure. The treated supernatant is recirculated back to the WWTP headworks.

A monitoring campaign was conducted in the sidestream line at Carbonera WWTP treatment plant for approximately 4 months (January 2019–April 2019). Dissolved N_2O concentrations were measured using a polarographic Clark-type electrode (Unisense, Aarhus, Denmark). To supplement the long-term monitoring campaign with Unisense probes, N_2O emissions in the headspace of the SBR reactor, were also continuously monitored with MIR9000CLD analyser (Environment Italia S.p.A.) during March–April 2019. Details of the monitoring campaign, N_2O emissions' calculation and laboratory analyses are provided in the supplementary material (S1–S3).

2.2. Data analysis

2.2.1. Methodological framework

Fig. 2 summarises the methodological framework of the study. Phase one includes preliminary analysis of the collected data. Features extraction and density-based clustering was applied (Ester et al., 1996), to isolate abnormal cycles. The methodology and results of abnormal cycles' isolation are given in the supplementary material (section S4). In phase two, the behaviour of N_2O emissions and dissolved N_2O concentration during normal operation was investigated; efforts were focused to identify dependencies with the operational dataset and laboratory analyses. Finally, in phase three, classification and regression models were trained to predict the behaviour of aerobic dissolved N_2O concentration in the different cycles. Support vector machine classification (SVM) and regression (SVR) models were constructed (Cortes and Vapnik, 1995).

The first step for the prediction of the average aerobic dissolved N_2O concentration included the training of an SVM classifier (ANOXSVM) to predict whether dissolved N_2O will be consumed during the anoxic phase. This was significant, given that accumulated dissolved N_2O in the beginning of the aerobic phase, will be stripped during aeration. All cycles were divided in two classes: class anoxA (dissolved $N_2O < 0.6$ mg/L) and class anoxB (dissolved $N_2O > 0.6$ mg/L). The dissolved N_2O concentration threshold was set equal to 0.6 mg/L, since in ~88% of these cases, N_2O was consumed by the end of subsequent anaerobic phase. In cycles belonging to class anoxA, no N_2O carryover was assumed. It is important to note that the term anaerobic phase, is used to describe the first operational phase of the SBR (Fig. 1) within each cycle and is not necessarily representative of the actual conditions in the reactor.

Subsequently, an SVM classifier (ANSVM) was trained to predict if dissolved N_2O will be consumed in the subsequent anaerobic phase. The threshold of N_2O at the end of the anaerobic phase was set equal to 2.6 mg/L (sensor calibration limit). Therefore, anaerobic phases with accumulated N_2O were classified in two groups: class anaerA (N_2O concentration < 2.6 mg/L) and anaerB (N_2O concentration > 2.6 mg/L). Cycles belonging to anaerA class, were used to train an SVR model (ANSVR) to predict the dissolved N_2O concentration at the end of the anaerobic phase.

Finally, an SVR model was trained to predict the average N_2O concentration during the aerobic phase (AERSVR), utilizing the ANSVR model predictions for cycles with initial aerobic N_2O less than 2.6 mg/L. Finally, the aerobic SVR model was also tested to cycles belonging in class anaerB (N_2O concentration > 2.6 mg/L). In anaerB cycles, initial aerobic N_2O accumulation exceeds the calibration limit of the sensor. Additionally, aerobic N_2O accumulation starts before completion of the stripping of pre-existing dissolved N_2O. In these cases, the average dissolved N_2O concentration of the cycle, was calculated considering the period from the first minimum of dissolved N_2O concentration until the end of aeration (or after 30 min if a local minimum did not exist). Additionally, initial N_2O accumulation was assumed to be equal to 0.6 mg/L (average minimum after initial N_2O stripping observed in these cycles).

In practice, the methodology followed was not linear as it is illustrated in Fig. 2; it involves several backward and forward loops between the different steps. The feedback loops were necessary to leverage the knowledge discovered and adjust the data-preparation (i.e. new features extraction, different pre-processing) and mining phases.

2.2.2. Support vector machines classification and support vector regression

Support vector machines (SVMs) are a range of supervised non-parametric classification and regression algorithms that have various applications in several fields including hydrology (Raghavendra and Deka, 2014), bioinformatics (Byvatov and Schneider, 2003) and wastewater (Corominas et al., 2018). For instance, in wastewater, support vector regression (SVR) has been successfully applied to data generated from mechanistic modelling of biological processes (Fang et al., 2011) or to experimental data (Seshan et al., 2014) to predict reactors' performance.

SVM classification and SVR models were constructed to predict the behaviour of dissolved N_2O production/consumption in different phases of the SBR operation (Fig. 2). SVM aims to define an optimum separating hyperplane in the feature space that maximizes the margin between two different classes. Classes with large margins are clearly separable and provide a 'safety' for the generalisation of the algorithm when applied to new points. In practical applications, the overlapping of a number of data belonging to the two classes, is common. Therefore, soft margins are introduced to allow a number of misclassifications to identify feasible solutions when the training dataset is not strictly linearly separable. Similarly, in the SVR case, the aim of the method is to identify the hyperplane that has the minimum distance to all data points. A complete description of the SVM and SVR algorithms is provided in the supplementary material. Radial basis function (RBF) is a widely used kernel function and was selected to construct the models in this study. The 'kernel trick' enables SVMs to operate even in infinite feature space (where data are mapped), without in practice executing calculations there (Luts et al., 2010).

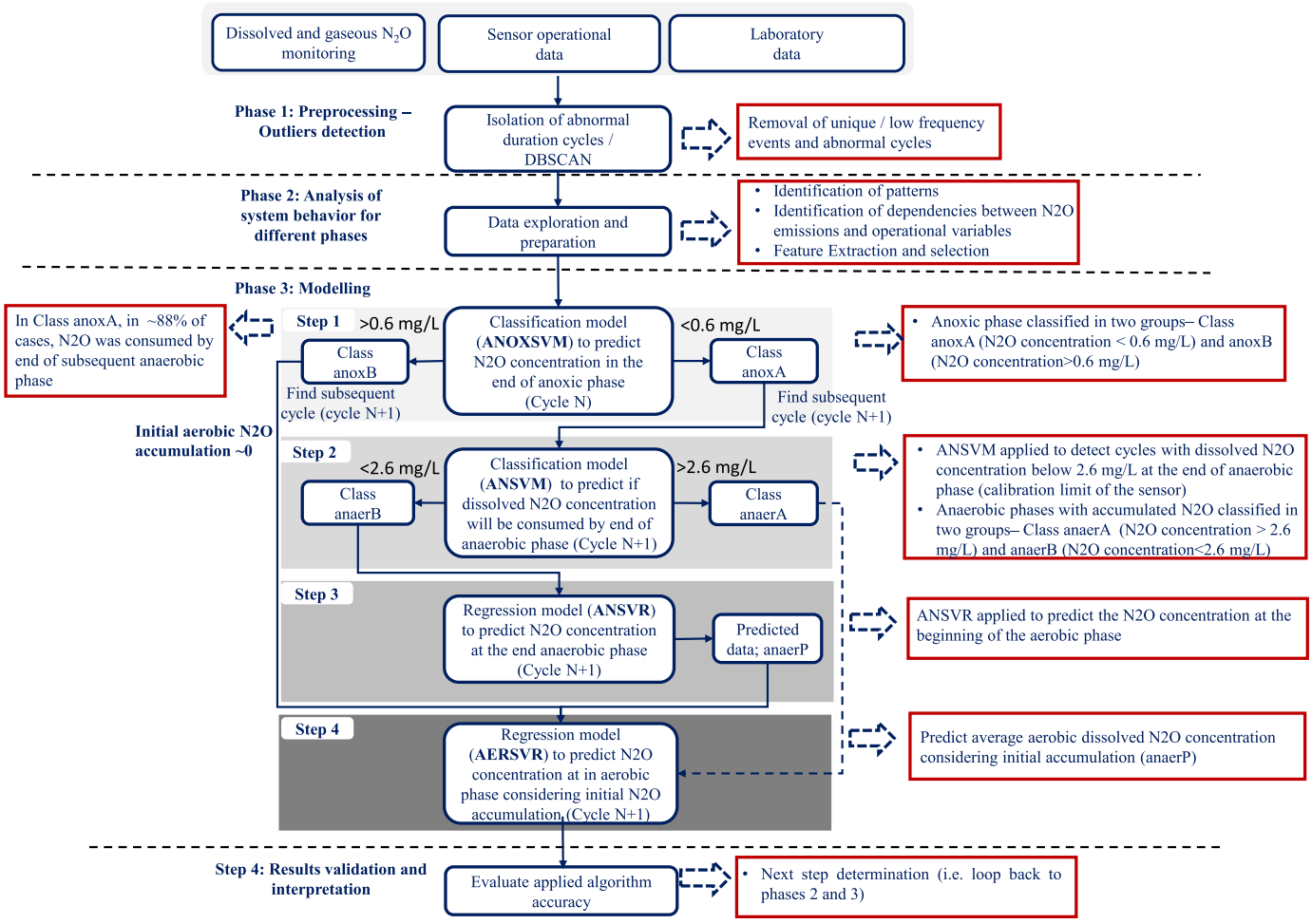

Fig. 2. Methodological Framework followed in the study.

The algorithms were implemented with the kernlab package (Karatzoglou et al., 2004) in R software. Repeated 10-fold cross validation (3 repetitions) was applied to select the cost and gamma (γ) regularization parameters over a grid-search with the caret package (Kuhn, 2008). The cost determines the penalty of misclassified instances or instances violating the maximal margin whereas γ determines the amplitude of the kernel. The dataset was randomly divided into test and train, with 70% of the available data used for training the SVM model and 30% used for testing.

In the classification case, over-sampling was applied for the minority classes within the 10-fold cross validation loop (before training). Local models were developed based on observations from each phase of the SBR reactor instead of the dataset from the duration of the whole cycle. The underlying characteristics and dependencies of the operational variables vary between anoxic, aerobic and anaerobic conditions. Additionally, the performance of the system under different phases within the cycle can also vary. There are significant benefits in the development of local phase-based models. The behaviour of dissolved N_2O and triggering operational conditions vary between the different phases; local models enable to investigate the phase-based dependency structures that would not be possible using the whole cycle dataset. The performance of the classification SVM models were evaluated based on accuracy and kappa and from the sensitivity and specificity as described in the supplementary material (S3.1). Similarly, the regression models were evaluated considering the root mean squared error (RMSE) and R-squared (R^2) (S3.1).

3. Results and discussion

3.1. SCENA performance

The SBR treats up to 43 kg of N/day of anaerobic supernatant, which results in a volumetric nitrogen loading rate up to 0.62 kgN/m^3 day. The performance of the SBR reactor in terms of NH_4–N removal, was stable during the monitoring campaign. During system's normal operation (January 2019–April 2019), the average removal efficiency of NH_4–N, TN and PO_4–P was 78%, ~77% and 78% respectively. Influent and effluent concentrations of the SCENA system for the duration of the monitoring campaign are provided in Table 1. A detailed description of the abnormal cycles isolated is provided in the supplementary material.

3.2. N_2O emission factor

N_2O emissions were measured using a gas analyser (March–April 2019); on average ~0.8 kg of N_2O–N was emitted in each cycle, equivalent to 7.6% of the NH_4–N load in the SBR. In terms of the NH_4–N removed the N_2O EF was equal to 11% (±4). The emissions during the aerobic phase were considered. N_2O emissions exhibited significant variability ranging from 0.14 kg N_2O–N/cycle (1.3% of NH_4–N load) to ~2 kg N_2O–N/cycle (19% of NH_4–N load) as

Table 1
Influent and effluent concentrations of the SCENA system.

	Parameter	unit	mean	Sd
SBR Influent	NH_4–N	mg/L	992.5	90
	PO_4–P	mg/L	30.8	6.9
	pH		8.2	0.2
	sCOD	mg/L	1111.7	562
	Flow-rate	m^3/d	30 (8.4 per cycle)	2.2
	Air flow-rate	m^3/h	450 (170–520)	78
	Dimensions	mxmxm	8 x 3.5 x 2.5	
SBR Effluent	NH_4–N	mg/L	214.7	80.93
	NO_2–N	mg/L	3.23	9.7
	NO_3–N	mg/L	0.28	0.34
	PO_4–P	mg/L	6.78	2.22
	pH		8.04	0.3
SBR Reactor	MLSS	g/L	5.05	0.87
	HRT	d	2.39	0.18
	SRT	d	13 -15	
	pH		7.7	0.5
	T	°C	30.02	1.56
Fermentation Liquid	NH_4–N	mg/L	715	72.6
	PO_4–P	mg/L	86	12
	pH		5.6	0.6
	T	°C	36	5.1
	sCOD	mg/L	13082	2228
	ferm_Hac	mg/L	3250	546
	ferm_HPr	mg/L	2281	588
	ferm_Hbut	mg/L	1347	196
	Flow-rate to SBR	m^3/day	7.45 (~2.41 per cycle)	3.0

shown in Fig. 3 (a). Emission peaks higher than 1.5 kg N_2O–N/cycle and the increasing trend observed close to the end of the monitoring campaign coincide with peaks in the conductivity change in the aerobic phase of the cycles (Fig. 3 (b)). Laboratory analyses performed approximately four times per week, did not demonstrate any significant changes in the influent COD, NH_4–N loads and removal efficiencies linked with the increasing trend of the emissions observed in Fig. 3 (a). Given the wide range of the N_2O emissions observed in the system, in the following sections, efforts were focused to identify triggering operational conditions.

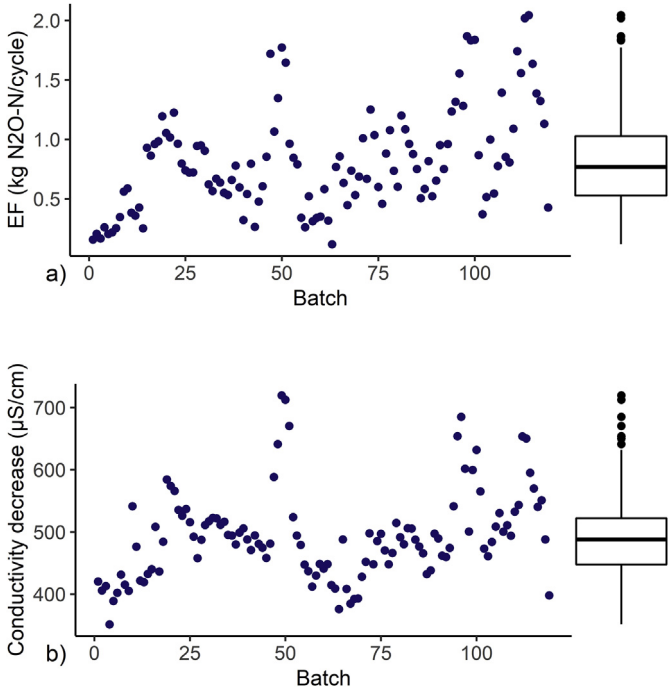

Fig. 3. (a) N_2O emissions and (b) aerobic phase conductivity decrease, during monitoring campaign (gas analyser, March–April).

3.3. Energy consumption vs N_2O emissions

The operational carbon footprint of the sidestream line was estimated using the direct GHG emissions (from N_2O) and electricity consumption. The electricity consumption was relatively steady over the monitoring period; on average ~5.4 kWh was consumed in the SBR for the removal of 1 kg of NH_4–N from the anaerobic supernatant. The average energy consumption of the SBR represented ~77% of the total electricity consumption of the SCENA system. On average ~48.7 kg of CO_{2eq} are generated for the removal of 1 kg of NH_4–N due to the direct N_2O emissions and electricity consumption in the system. The contribution of the total N_2O emissions to the operational carbon footprint of the SCENA process ranged from 66.7% to 96.8% when all the equipment electricity consumption (i.e. fermenter, dynamic thickener) were considered. Given the variability of the N_2O emissions observed in the system (Fig. 3) the kg of CO_{2eq} emitted per kg of NH_4–N removed ranged between 9.5 kg CO_{2eq} to 117.7 kg CO_{2eq}. Fig. 4 (a), shows the average operational carbon footprint (considering direct N_2O emissions and electricity consumption) of the SCENA system for two cases with different ranges of N_2O emissions. In the first case (26/03), a considerable amount of N_2O was emitted, equal to ~10.5% of the influent NH_4–N load. In the second case, the emissions were significantly lower, equal to ~4% of the influent NH_4–N load. Both cases are characterised by similar influent NH_4–N concentrations, phase duration, temperature and ammonia removal efficiencies (~79%). The DO concentration is equal to ~1 mg/L. In case 1, the operational carbon footprint of the process is ~136% higher compared to case 2. This example shows that under similar conditions (considering laboratory analyses, average pH and DO), dissolved N_2O concentrations can vary significantly in the studied system. Investigation of the behaviour of conductivity during the

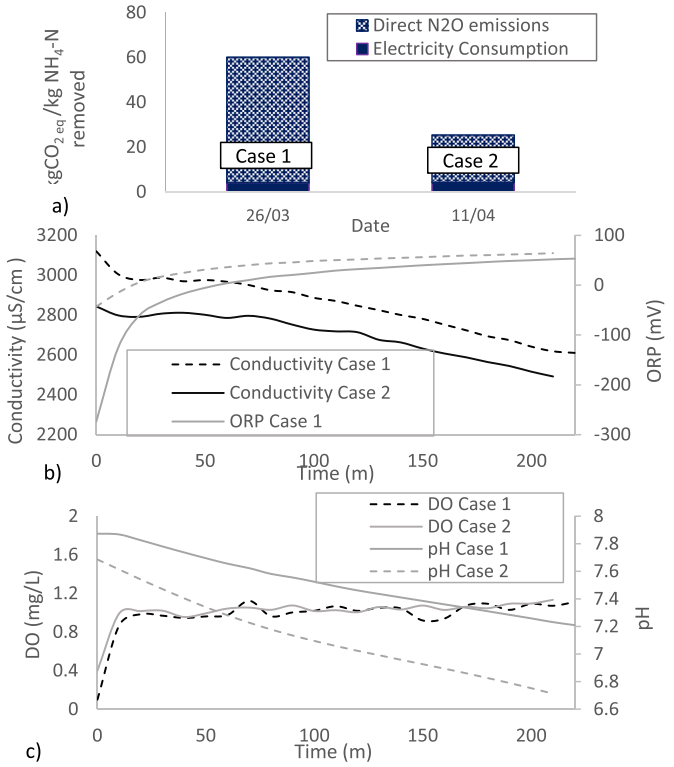

Operating Conditions	Unit	26/03	11/04
Influent NH_4-N	mg/L	1186.3	1154.13
DO	mg/L	1.0	1.0
Anaerobic/Aerobic/ Anoxic duration	h	0.5/3.6/1.5	0.5/3.7/1.5
Effluent NH_4-N	mg/L	211.1	185.9
Effluent NO_2-N	mg/L	~0	1.6
Temperature	°C	31.7	32.1

Fig. 4. (a) Example of the effect of N_2O emissions in the operational carbon footprint for two cases, (b) aerobic profiles of conductivity, ORP and (c) DO for the two cases shown in (a).

two aerobic phases, showed higher conductivity and pH decrease in case one (~510 μS/cm and ~1 respectively) compared to case two (~350 μS/cm and 0.7 respectively) (Fig. 4(b) and (c)). Additionally, the initial aerobic ORP in case 2, was higher (−43 mV) compared to case 1 (−274 mV) (Fig. 4 (b)). Therefore, efforts to understand the N_2O triggering operational conditions and mitigate GHG emissions, should consider the dynamic in-cycle behaviour of the variables monitored in the system. The relationship between the operational variables (i.e. DO, NH_4—N concentration, ORP, conductivity) will be discussed in the following sections.

3.4. Variability of N_2O emissions during normal operation

N_2O was emitted during aeration phase in all cycles and correlated significantly with the dissolved N_2O accumulation. One representative cycle profile for the dissolved N_2O concentration and N_2O emissions in cycles starting without dissolved N_2O accumulation from the previous cycle is shown in Fig. 5, together with the DO, NH_4—N, conductivity, ORP and pH.

ORP at the beginning of the aerobic phase shows a correlation with the DO, whereas N_2O accumulation is minimum. Dissolved N_2O increases in the first 60—70 min of aeration (a small change in the pH slope can be seen coinciding with the peak of accumulated N_2O) indicating that the generated N_2O is higher than the stripped N_2O. N_2O accumulation shows a decreasing trend after ~90 min of aeration. Subsequently dissolved N_2O concentration increases when aeration stops, and the anoxic phase starts. This shows that production of N_2O continues under decreasing DO and until DO depletion. The calibration range of the dissolved N_2O probe is between 0 and 2.6 mg/L. Therefore, the accumulation of dissolved N_2O can be higher than the peak shown in Fig. 5. During the anoxic phase, pH increases rapidly during the dosage of fermentation liquid, followed by a slow decrease upon the end of carbon dosage phase. A sudden change in the ORP signal slope ("nitrite knee") indicates the depletion of nitrite whereas TN still exists in the form of N_2O. Accumulated N_2O is subsequently depleted rapidly after NO_2—N depletion.

3.5. The pattern of N_2O emissions

Offline data from laboratory studies and the ranges of the operational variables were analysed in order to investigate significant changes that contribute to high accumulation of dissolved N_2O concentration and high N_2O emissions.

Fig. 6 (a) shows the daily average dissolved N_2O concentration (coloured points) during aerobic phase versus conductivity at the end of aerobic phase and the effluent NH_4—N concentration. Conductivity is significantly related and can be linked with the NH_4—N concentration in the reactor (spearman correlation coefficient equal to 0.97). High average aerobic dissolved N_2O concentration (>1.5 mg/L) was mainly observed with NH_4—N concentrations lower than 150 mg/L and higher than 300 mg/L in the effluent of the SBR. Additionally, the spearman correlation coefficient between dissolved N_2O and average aerobic conductivity decrease rate (μS/cm/min) was equal to −0.7 and N_2O concentration peaks were observed for conductivity decrease rate > 1.8 μS/cm/min. The latter indicates that higher emissions occur under high ammonia removal efficiency that can be linked with higher ammonia oxidation rates (AOR) (i.e. due to pH values observed ~8) triggering the NH_2OH oxidation pathway or higher than average NO_2^-N accumulation (triggering nitrifier denitrification pathway). Domingo-Félez et al. (2014) found that N_2O production rates were positively correlated with the extant nitrification rate in a single-stage nitritation/Anammox reactor. Similarly, Law et al. (2011) identified a linear relationship between AOR and N_2O emissions in a partial nitritation SBR reactor treating the reject water from anaerobic digestion. Law et al. (2011) suggested that is attributed to higher accumulation of the ammonium oxidation intermediates (hydroxylamine (NH_2OH) and nitrosyl radical (NOH)) leading to faster N_2O formation or to the increased use of electrons reducing nitrite to nitric oxide (nitrifier denitrification pathway) under low DO concentrations. High nitrite accumulation has been also linked with elevated N_2O emissions and the nitrifier denitrification pathway, especially under low DO concentrations (Tallec et al., 2006; Kampschreur et al., 2008; Desloover et al., 2011; Peng et al., 2015; Massara et al., 2017; Law et al., 2012). For instance, Peng et al. (2017) and Kampschreur et al. (2009), in a nitritation-denitritation SBR and a full-scale single stage nitritation-Anammox reactor respectively, identified linear relationship between nitrite accumulation and N_2O emissions at DO levels below 1.5 mg/L. Similarly, Tallec et al. (2006) in a nitrifying activated sludge observed eightfold increase of N_2O emissions with the addition of nitrite pulses (10 mg/L) at DO equal to 1 mg/L. Therefore, both hydroxylamine oxidation and the nitrifier denitrification are possible during aeration in the investigated SBR.

The average dissolved N_2O concentration during the aerobic phase of different cycles varied significantly in relation to the average DO concentration. Fig. 6 (b), shows that the dissolved N_2O

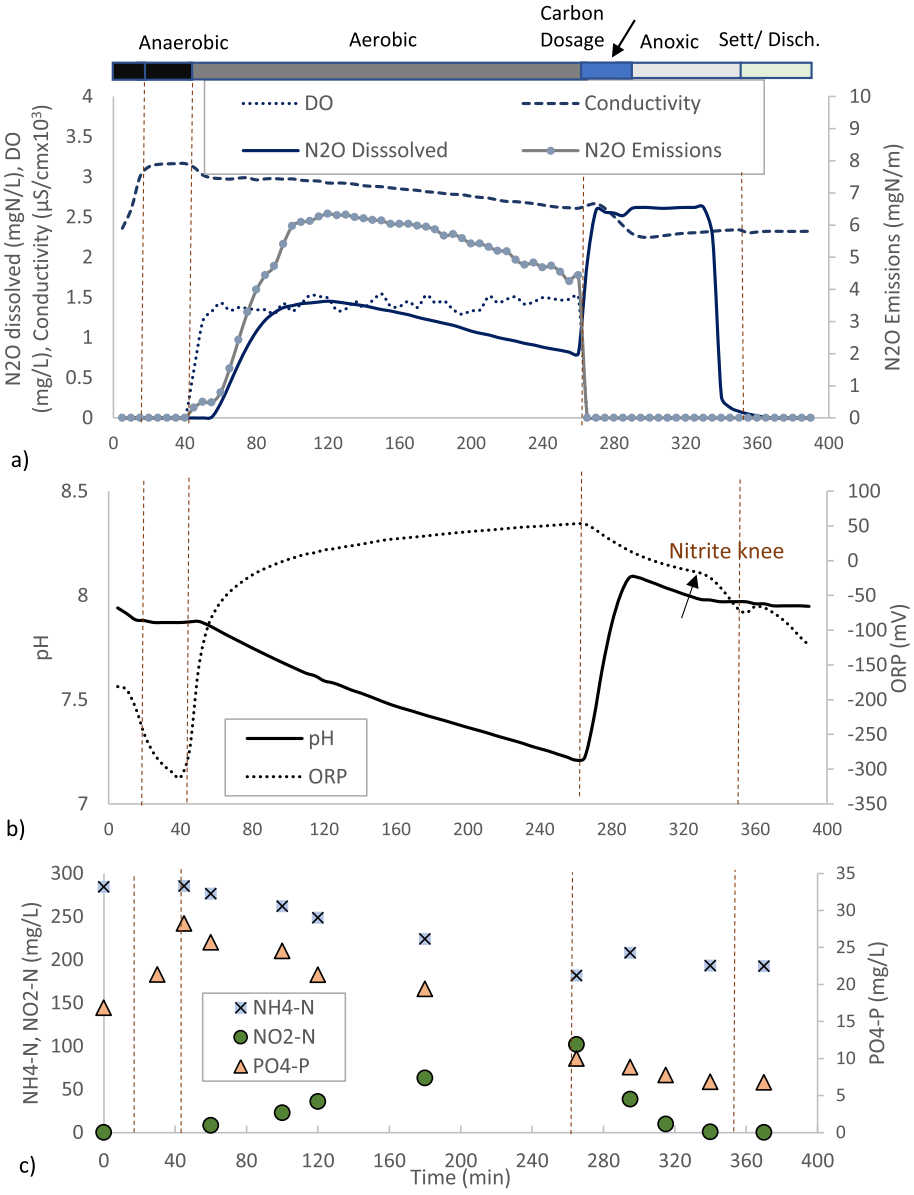

Fig. 5. Representative cycle profile for the (a) dissolved N_2O concentration, N_2O emissions, conductivity, DO, (b) ORP and pH, and (c) NH_4—N, NO_2—N and PO_4—P concentrations.

concentration peaks coincided with average DO concentrations less than 0.9–1 mg/L. The spearman correlation coefficient between dissolved N_2O and DO concentrations was equal to −0.7. The coloured points in the Figure, represent the ORP at the end of the aerobic phase; ORP is higher than 40 mV in the majority of the cycles with average aerobic dissolved N_2O concentration less than 1 mg/L. Only cycles without dissolved N_2O accumulation from the previous anoxic phase are shown in the graph. Stenström et al. (2014) showed decreasing DO concentrations lower than 1–1.5 mg/L are linked with higher nitrite accumulation and are positively correlated with N_2O emissions during nitrification in a full-scale predenitrification-nitrification SBR treating anaerobic supernatant. Similarly, Pijuan et al. (2014) reported an increase of N_2O emissions in a nitritation reactor with the reduction of DO from 4 to <1 mg/L. During the monitoring period, blowers operated at maximum flow-rate. Therefore, the presence of residual biodegradable COD concentration in the aerobic, is expected to decrease DO concentration. Similarly, higher influent NH_4^+ loads or higher ammonia oxidation rates (that can also result in increased NO_2^- accumulation) can impact the DO concentration in the system. The dissolved N_2O concentration can be affected by a combination of variables; therefore, it cannot be deduced that the decreased DO is the sole contributing factor triggering the increased N_2O generation observed.

3.6. Impact of accumulated N_2O in the end of anoxic and anaerobic phase

Several parameters have been reported to affect the N_2O accumulation under anoxic conditions, such as the inhibition of the nitrous oxide reductase (Nos) by free nitrous acid (FNA) or high accumulation of NO_2^-, the electron competition between electron acceptors and the type of carbon source (Itokawa et al., 2001; Pan et al., 2013; Zhou et al., 2008; Zhu and Chen, 2011). Additionally, low values of COD/N can result in incomplete denitritation and therefore, N_2O accumulation via the heterotrophic denitrification

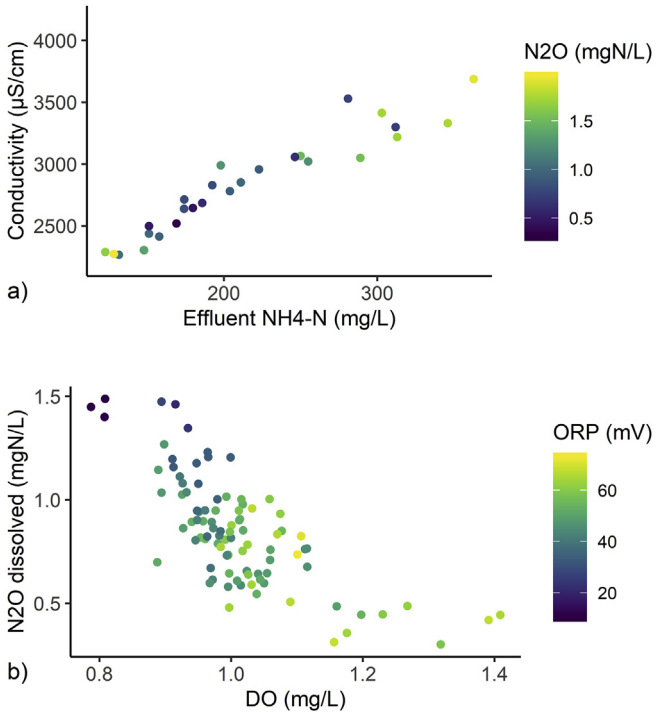

Fig. 6. (a) Daily average conductivity at the end of the aerobic phase versis effluent NH_4–N concentration (coloured points: average dissolved N_2O accumulated in the aerobic phase), (b) Aerobic average accumulated dissolved N_2O in respect to DO concentration; only cycles without initial N_2O accumulation from the previous anoxic cycle are shown (coloured points: ORP at the end of the aerobic phase).

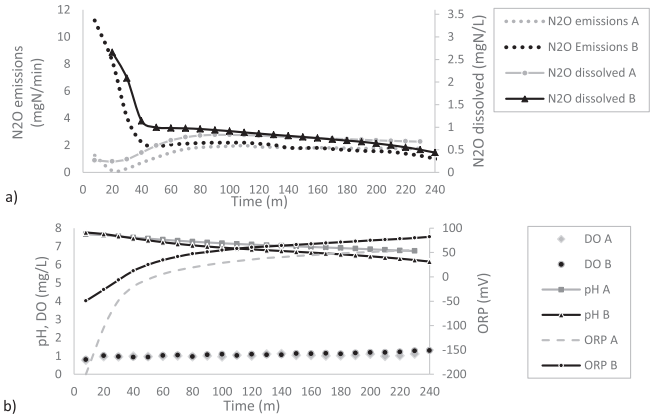

Fig. 7. (a) Representative profiles of dissolved N_2O concentration based on different initial concentrations of N_2O in the beginning of the aerobic phase and (b) ORP and DO profiles.

pathway during the anoxic phase of the SBR. Accumulated N_2O in the end of the anoxic phase is stripped in the subsequent cycle, increasing the N_2O emissions. Caranto et al. (2016) have recently showed that N_2O can be the main product of anaerobic NH_2OH oxidation catalysed by the cytochrome P460 in N. europaea. The latter can be an evidence of the biological N_2O generation under limited DO and high NH_3 concentrations, both conditions occurring in the target system in the during the transition from aerobic to anoxic phases when N_2O accumulation rapidly increases.

In this study, the average soluble COD concentration in the fermentation liquid was equal to 13082 mg COD/L over the monitoring period (Table 1). Overall, in >27% of the examined cycles the N_2O was completely consumed by the end of the anoxic phase. Zhu and Chen (2011), showed that the use of sludge alkaline fermentation liquid as carbon source in an anaerobic-aerobic system treating high-strength stream, can reduce the N_2O production by up to 68.7% compared to alternative carbon sources (i.e. acetic acid). On the other hand, Li et al. (2013a) in a process utilizing PHA as internal carbon source, observed higher N_2O production and reduction rates at higher influent COD concentrations linked with higher anaerobic PHA synthesis (ranging from 100 to 500 mg/L). The higher N_2O production rates were attributed to the accumulated NO_2^- inhibiting the N_2O reduction.

The dissolved N_2O concentration in the anoxic phase exceeded the calibration limit of the sensors; only cycles in which "nitrite knee" was observed and N_2O reduced to values lower than 2.6 mg/L could be investigated. Therefore, the effect on NO_2^- in anoxic N_2O generation could not be studied. However, studies have shown that elevated NO_2^- concentrations during denitrification can reduce the denitrification rate and increase the N_2O accumulation (Schulthess et al., 1995). The electron competition between nitrite reductase NIR, nitric oxide reductase (NOR) and nitrous oxide reductace (NOS) is intensified under high NO_2^- concentrations; NOS is less competitive under limitation of electron donor and this will result in N_2O accumulation (Pan et al., 2013; Ren et al., 2019).

Based on the profiles shown in Fig. 5, N_2O was always consumed after the depletion of NO_2^- during denitritation; specifically, dissolved N_2O concentration decreased after the "nitrite knee". Gabarró et al. (2014), studied a partial-nitritation reactor treating landfill leachate, and operated under alternating aerobic/anoxic conditions to allow heterotrophic denitritation. The authors demonstrated that significant N_2O accumulation was observed during anoxic periods. NO_2^- denitrification rate was higher under both biodegradable COD limiting conditions and after acetate addition compared to N_2O reduction; N_2O reduction rate was maximum after NO_2^- removal (similar to what was observed in this study). In denitrifying phosphorus removal processes, Li et al. (2013)a,b showed that the N_2O accumulation can be higher compared to conventional denitrification; the authors suggested that in the electron competition between denitrifying enzymes and PHA, N_2O reductase is less competitive. On the other hand, Ribera-Guardia et al. (2016) investigated the electron competition during denitrification (PHA as the sole carbon source) of enriched dPAO and dGAO biomass and found that higher N_2O accumulation in the latter culture. Additionally, the last step of denitrification was inhibited in dGAO cultures (N_2O accumulation up to ~84% of the N-reduced), under high levels of NO_2^- (~15 mgN/gVSS) whereas N_2O consumption in dPAO biomass was not affected. Wang et al. (2015) demonstrated that during denitrifying phosphorus removal, mitigation of NO_2^- accumulation is possible via continuous dosage of phosphate and nitrate. Wang et al. (2011), showed that optimisation of the synthesis of PHA during the anaerobic phase can mitigate the N_2O production during the anoxic phase leading to complete denitrification.

In the system, N_2O emissions and dissolved N_2O concentration in the aerobic phase is strongly related with incomplete denitritation in the previous cycle. In ~26% of the cycles with incomplete denitritation, the N_2O concentration did not decrease below ~2 mg/L in the anaerobic phase and therefore the stripping of accumulated N_2O in the subsequent aerobic phase was substantial. Fig. 7 (a) shows representative profiles of the dissolved N_2O concentration and the N_2O emissions based on different initial concentrations of N_2O in the beginning of the aerobic phase. The profiles of the ORP, DO and pH are comparable in the preseted cycles (Fig. 7 (b)). In cycle B ~0.56 kgN of N_2O were emitted during the aerobic phase, whereas in cycle A N_2O emissions are equal to 0.33 kgN (given the

duration of these cycles is not equal only 220 min were considered). The initial dissolved N_2O concentration in cycles A and B is equal to 0.27 and > 2.6 mg/L respectively. The N_2O emissions increased significantly due to the accumulated N_2O at the beginning of the previous anoxic phase that was stripped at the beginning of aeration.

Overall, in ~72% of the cycles, the dissolved N_2O concentration at the beginning of the anaerobic phase was higher than 0.3 mg/L. In cycles with dissolved N_2O concentration higher than 0.3 mg/L at the beginning of the anaerobic phase, the change in dissolved N_2O concentration during the anaerobic phase was highly correlated with the ORP at the beginning of the anaerobic phase. Additionally, the spearman correlation coefficient between the magnitude of the ORP reduction and magnitude of the dissolved N_2O reduction was equal to 0.7. Fig. 8 shows the boxplots of dissolved N_2O reduction in relation to initial anaerobic ORP and ORP change for two cases: i) negligible dissolved N_2O change mainly due to influent dilution or anaerobic dissolved N2O concentration >2.6 mg/L, and ii) occasions with N_2O reduction during the anaerobic phase. In Fig. 8 (a) only occassions with ORP decrease higher than −50 mV are shown. The presence of nitrites in the bulk liquid during the (anaerobic) phase affected the ORP. NO_2−N depletion in the bulk liquid resulted in a sharp "nitrite knee" in the ORP profile (similar to the one observed during the anoxic phase. Therefore, higher ORP change was expected in cycles with NO_2−N depletion and N_2O consumption during the anaerobic phase.

Anaerobic phase term, is used to describe the first operational phase of the SBR (Fig. 1) within each cycle and might not represent the actual conditions in the reactor. For instance, ORP ~ −80 mV in the anaerobic phase of the SBR indicates anoxic conditions, due to residual NO_2^-N concentration from the previous anoxic phase of the reactor.

3.7. Prediction and control of N_2O accumulation in the anoxic and anaerobic phases

As discussed in section 3.6, the behaviour of ORP was significantly related with the behaviour of NO_2^- and consequentially of the dissolved N_2O concentration during the anaerobic phase. Therefore, in the ANSVM model, features related with the ORP profile were mainly used (Table 2). Similarly, there was a strong link with the ORP behaviour and the "nitrite knee" with the N_2O accumulation during the anoxic phase. The features considered in ANOXSVM model are shown in Table 2.

The classification matrices for train and test datasets of the ANSVM and ANOXSVM models are presented in Table 3. The average classification accuracy for the ANOXSVM model, was equal to 99% and 97% for the test and validation datasets. Similar results were obtained for the anaerobic phase with 95% and 98% accuracy in the train and test datasets respectively.

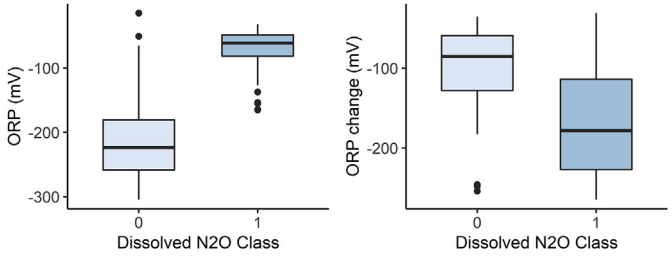

Fig. 8. Box-plots of the (a) initial anaerobic ORP and (b) the ORP change during the anaerobic phase for cycles with and without N_2O consumption (Class 0: no significant N_2O consumption or anaerobic N_2O concentration > 2.6 mg/L; Class 2: significant N_2O consumption).

Jaramillo et al. (2018) developed an SVM classifier to estimate online the end of partial nitrification in a laboratory aerobic-anoxic SBR based on features extracted from pH and DO sensors over time-windows, resulting in 7.52% reduction in the operational time. In this study, the main focus was to estimate offline the behaviour of N_2O emissions based on historical batch data. The results from this study indicate that ORP and pH sensor data can be used to detect the consumption of N_2O during the nitritation/nitrification in SBR reactors. The results show that knowledge-based feature-extraction and SVM classification could help in explaining the behaviour of the system and potentially optimise the control to consider the consumption of accumulated N_2O (i.e. in this system the denitritation can be stopped after the local maximum of the ORP rate after the "nitrite knee" in all the cycles investigated.)

Fig. 9(a) and (b) illustrate the predicted and measured N_2O concentration at the end of the anaerobic phase (ANSVR model). The SVR parameters were optimised based on the root mean square error using the train dataset. RMSE of the SVR model was equal to 0.11 and 0.1 mg N_2O−N/L for the train and test datasets respectively (R-squared equal to 0.85 and 0.75 respectively). As shown in Fig. 9 (b) the simulation results follow the behaviour of the actual dissolved N_2O concentrations observed. One of the major factors affecting the performance is the limited number of data points, but the prediction is still accurate.

3.8. Prediction of the N_2O concentration in aerobic phase

The input features are shown in Table 4 and were selected based on the identified influential variables. The N_2O predicted values of the ANSVR model were used (anaerP). The procedure followed for the selection of model parameters was similar to the respective one followed for the anaerobic phase. Additionally, ANSVR test dataset cycles, were identified and used in AERSVR test dataset A. The model was also applied in anaerB cycles (test dataset B).

Fig. 10 (a), shows the predicted and measured average aerobic N_2O concentration for the trained and test datasets. RMSE of the SVR model was equal to 0.06 and 0.11 mg N_2O−N/L for the train dataset and test dataset A respectively, whereas the R-squared was equal to 0.94 and 0.82 (Fig. 10(a) and (b)).

The RMSE of the predicted values for the test dataset B, was equal to 0.29 mg N_2O−N/L and the R-squared was equal to 0.72 (Fig. 10 (a)). The AERSVR model underpredicted the average dissolved N_2O concentration of test B dataset. This is expected given that in test B dataset cycles, the initial aerobic N_2O accumulation exceeds the sensor calibration limit. Therefore, on many occasions the initial aerobic N2O accumulation was also underestimated (section 2.2.1 - anaerB cycles). An example is shown if Fig. 11. In cycle A, the average dissolved N_2O concentration (calculated as discussed in section 2.2.1 for anaerB cycles) is equal to 1.33 mg/L. The AERSVR model predicted 0.87 mg/L underestimating the actual concentration (considering initial accumulation equal to 0.6 mg/L). In cycle B, the AERSVR model predicted N_2O concentration equal to 0.61 mg/L (considering initial accumulation equal to 0.6); the observed average dissolved N_2O concentration (after the local minimum), was equal to 0.6 mg/L.

The results show that under the investigated operational conditions, the framework shown in Fig. 2 can provide a good estimation of the real dissolved N_2O behaviour and concentration observed during the different phases of SBR operation. Instabilities in the performance of machine learning models due to changes in the operational conditions in wastewater bioreactors have been reported in the literature (Shi and Xu, 2018). Therefore, long-term datasets and investigation of different patterns and dependencies should be investigated before model construction.

Table 2
Features used in the classification algorithm to predict the accumulation of dissolved N_2O at the end of the anoxic and anaerobic phases.

Anaerobic	Anoxic	Anaerobic regression
ORP phase initial	Last ORP value	ORP phase initial
ORP change	ORP change	ORP change
First local maximum ORP first derivative	Mean pH	
Local minimum of ORP first derivative after first local maximum ORP first derivative	Difference between first local maximum (after carbon dosage) and subsequent local minimum of the ORP first derivative	pH phase initial
Duration between first local maximum and subsequent local minimum of the ORP first derivative	Duration of carbon dosage	Time of ORP first derivative minimum/duration of phase
pH phase initial	Duration between first local maximum (after carbon dosage) and subsequent local minimum of the ORP first derivative	Difference between first local maximum and subsequent local minimum of the ORP first derivative
Time local minimum ORP first derivative/Phase duration	Last ORP first derivate	

Table 3
SVM classification results anoxic and anaerobic phases.

Phase	Dataset	Misclassified	Sensitivity	Specificity	Accuracy (%)	Kappa	Class
Anoxic phase cycle N	Train	anoxA: 1 anoxB: 0	1	0.99	99	0.97	anoxA: Final dissolved N_2O concentration end of anoxic < 0.6 mg/L anoxB: Final dissolved N_2O concentration end of anoxic > 0.6 mg/L
	Test	anoxA: 1 anoxB: 0	1	0.98	98	0.92	
Anaerobic phase cycle N+1	Train	anaerA:2 anaerB: 1	0.98	0.97	97	0.94	anaerA: N_2O end of anaerobic > 2.6 mg/L
	Test	anaerA: 1 anaerB: 0	1	0.97	98	0.95	anaerB: N_2O end of anaerobic < 2.6 mg/L

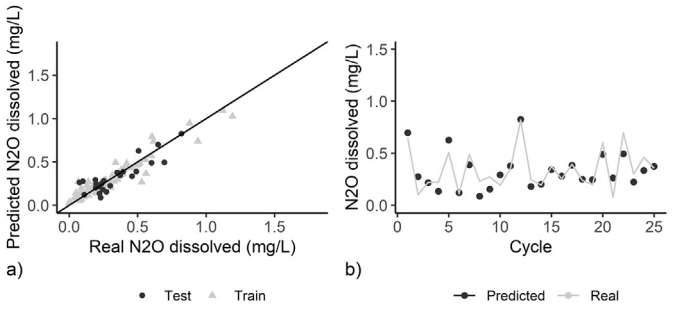

Fig. 9. (a) Predicted vs measured dissolved N_2O concentration in the end of the anaerobic phase (ANSVR) for the test and train datasets and (b) comparison of predicted and measured dissolved N_2O concentration for the test dataset.

3.9. Mitigation strategy

During aerobic phases, elevated average dissolved N_2O concentration was linked with DO less than 1 mg/L and increased conductivity decrease rates (conductivity values represent NH_4–N concentration values in the reactor). Therefore, cycles with increased conductivity decrease rate indicate higher NH_4–N removal efficiency and NO_2^-N accumulation. Dissolved N_2O concentrations lower than 0.6 mg/L were identified in cycles with average DO concentration equal to ~1.36 mg/L, and conductivity decrease rate >1.8 μS/cm/min. Increasing the reactor DO concentration to values higher than 1.3 mg/L can result in decreased aerobic N_2O generation (Law et al., 2012). However, with the current anaerobic supernatant feeding strategy, blowers operate at maximum flowrate, so it is not possible to increase the aeration in the system.

On the other hand, the implementation of a step-feeding strategy could foster the reduction of N_2O emissions thanks to the lower NH_4–N and free ammonia (FA) concentration at the beginning of the cycle, which has been recognized as a triggering factor for N_2O production (Desloover et al., 2012). Conductivity at the end of the cycle can act as surrogate to estimate the effluent NH_4–N concentration of the reactor and optimise the anaerobic supernatant feeding load. Consequently, the aerobic initial NH_4–N concentration could be controlled to avoid either FA accumulation or high AOR with subsequent N_2O generation.

Additionally, frequent alternation of aerobic/anoxic phases can be introduced in order to avoid high nitrite accumulation. The impact of nitrite concentration on N_2O production can be also minimized by ensuring adequate DO levels within the reactor to

Table 4
Features selected in the SVR model for the aerobic phase.

Aerobic Features
Average conductivity rate
ORP end of aeration
ORP increase during aeration
Conductivity at the beginning of aeration
Average DO
pH at the beginning of aeration
Conductivity increase (based on the conductivity at the end of the aerobic phase of the previous cycle)
pH change during aeration
Initial aerobicN_2O concentration (based on ANSVR predictions)

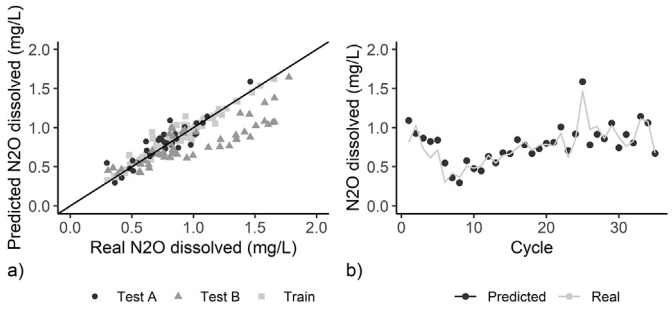

Fig. 10. (a) Predicted vs measured dissolved N2O concentration (AERSVR) in the aerobic phase for the train dataset, the test dataset A and the test dataset B and (b) comparison of predicted and measured dissolved N2O concentration for the test dataset B.

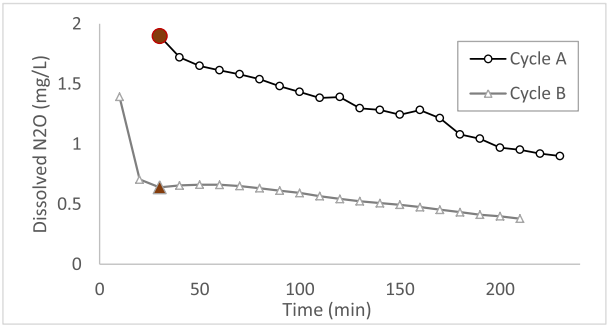

Fig. 11. An example of dissolved N2O profiles for cycles belonging to anaerB cycles (test dataset B). The red points represent the first point considered for the calculation of the average aerobic N_2O accumulation (as described in section 2.2.1). Data points in the beginning of aeration exceeding sensor calibration limits are not shown. (For interpretation of the references to colour in this figure legend, the reader is referred to the Web version of this article.)

inhibit the nitrifiers denitrification pathway (Blum et al., 2018; Law et al., 2013). Rodriguez-Caballero et al. (2015) reported that in a full-scale SBR treating municipal wastewater, intermittent aeration (alternation between 20 and 30 min oxic and anoxic) led to a minimisation of N_2O compared to long oxic periods that enhanced N_2O emission. The authors related this behaviour to the presence of shorter aeration times with subsequently lower nitrite accumulation and N_2O production.

In addition, Su et al. (2019) reported that slightly acidic or neutral pH in nitritation reactors (at values that do not inhibit microbial activity) can decrease N_2O generation by up to seven times. Based on the pH profiles observed in this study, regulation of aerobic (alkalinity consumption) phase duration can be also considered to control the pH at lower levels.

The developed models can be used to estimate rapidly and precisely the hard-to-measure N_2O concentrations during aeration and detect N_2O accumulation in non-aerated phases. Additionally, it can alert operators about cycles with anoxic and anaerobic N_2O accumulation and elevated aerobic N_2O concentrations, that require modifications to the system operation. The ANOXSVM model can predict if N_2O is consumed in anoxic phases or if anoxic duration should be extended. Thus, additional provision of fermentation liquid can be performed to promote N_2O consumption through denitritation, when after 70–90 min the anoxic SVM model still indicates incomplete denitritation.

This study provides evidence on the relationship of DO, ORP and conductivity and pH with the dissolved N_2O concentration (in terms of correlation coefficients, behaviour and thresholds that indicate specific ranges of N_2O accumulation). These findings together with the models developed in this study, can be the basis for the development of intelligent control algorithms to integrate emissions control in sidestream SBR reactors performing nitritation/partial nitritation or other systems similar to SCENA. Moreover, features based on ORP, pH, DO and conductivity measurements in wastewater SBR processes, that can be used to predict dissolved N_2O concentrations have been identified. The developed framework can be also tested in continuous processes for the data-driven prediction of N_2O emissions.

4. Conclusions

Knowledge discovery and data-mining techniques were employed to extract useful information about the dynamic behaviour of N_2O, and to predict the behaviour of dissolved N_2O concentration in a full-scale SBR reactor treating the anaerobic supernatant. The main conclusions are summarized as follows:

- The N_2O emissions in SCENA process varies from 1.3% to 19% of NH_4–N load, therefore they can contribute considerably to the operational carbon footprint of the process (~90% on average).
- Average aerobic dissolved N_2O concentration could significantly vary under similar influent loads, DO, pH and removal efficiencies. Extracting information from the dynamic in-cycle behaviour of the variables monitored in the system is a significant step towards understanding N_2O behaviour.
- Aerobic dissolved N_2O concentration peaks (>1 mg/L), were observed in cycles with average DO concentrations less than 0.9–1 mg/L and ORP concentration at the end of the aerobic phase less than 40 mV. Conductivity was correlated with the reactor NH_4–N concentration (0.97). N_2O peaks were also observed in cycles with elevated decrease of conductivity during aeration. Step-feeding, control of initial NH_4–N concentrations and control of pH via the regulation of aerobic phase duration can mitigate the N_2O peaks observed in this study.
- The accumulated N_2O at the end of the SBR anoxic phase was stripped in the subsequent aerobic phase and had a significant impact on the amount of N_2O emitted. The accumulated N_2O was consumed rapidly after “nitrite knee” that was linked with the nitrite depletion. The ANOXSVM model can be used to detect if anoxic duration should be extended or additional fermentation liquid provided to enhance N_2O consumption in anoxic phases.
- This study shows that low-cost sensors, conventionally used to monitor SBR systems (i.e. pH, DO, ORP), have good capabilities to predict the dissolved N_2O behaviour and concentrations when couple with knowledge discovery techniques. The AERSVR model, showed reliable estimations of the aerobic N_2O concentration and can provide guidance to WWTPs operators, on whether N_2O levels are acceptable or mitigation actions are required.

Declaration of competing interest

The authors declare that they have no known competing financial interests or personal relationships that could have appeared to influence the work reported in this paper.

Acknowledgements

This research was supported by the Horizon 2020 research and innovation program SMART-Plant (grant agreement No 690323).

Appendix A. Supplementary data

Supplementary data to this article can be found online at https://doi.org/10.1016/j.watres.2020.115799.

References

Blum, J.-M., Jensen, M.M., Smets, B.F., 2018. Nitrous oxide production in intermittently aerated Partial Nitritation-Anammox reactor: oxic N2O production dominates and relates with ammonia removal rate. Chem. Eng. J. 335, 458–466. https://doi.org/10.1016/j.cej.2017.10.146.

Byvatov, E., Schneider, G., 2003. Support vector machine applications in bioinformatics. Appl. Bioinf. 2, 67–77.

Caranto, J.D., Vilbert, A.C., Lancaster, K.M., 2016. Nitrosomonas europaea cytochrome P460 is a direct link between nitrification and nitrous oxide emission. Proc. Natl. Acad. Sci. Unit. States Am. 113, 14704–14709. https://doi.org/10.1073/pnas.1611051113.

Corominas, Ll, Garrido-Baserba, M., Villez, K., Olsson, G., Cortés, U., Poch, M., 2018. Transforming data into knowledge for improved wastewater treatment operation: a critical review of techniques. Environ. Model. Softw., Special Issue on Environmental Data Science. Applications to Air quality and Water cycle 106, 89–103. https://doi.org/10.1016/j.envsoft.2017.11.023.

Cortes, C., Vapnik, V., 1995. Support-vector networks. Mach. Learn. 20, 273–297. https://doi.org/10.1007/BF00994018.

Desloover, J., De Clippeleir, H., Boeckx, P., Du Laing, G., Colsen, J., Verstraete, W., Vlaeminck, S.E., 2011. Floc-based sequential partial nitritation and anammox at full scale with contrasting N2O emissions. Water Res. 45, 2811–2821. https://doi.org/10.1016/j.watres.2011.02.028.

Desloover, J., Vlaeminck, S.E., Clauwaert, P., Verstraete, W., Boon, N., 2012. Strategies to mitigate N2O emissions from biological nitrogen removal systems. Curr. Opin. Biotechnol., Energy biotechnology • Environmental biotechnology 23, 474–482. https://doi.org/10.1016/j.copbio.2011.12.030.

Domingo-Félez, C., Mutlu, A.G., Jensen, M.M., Smets, B.F., 2014. Aeration strategies to mitigate nitrous oxide emissions from single-stage nitritation/anammox reactors. Environ. Sci. Technol. 48, 8679–8687. https://doi.org/10.1021/es501819n.

Eskicioglu, C., Galvagno, G., Cimon, C., 2018. Approaches and processes for ammonia removal from side-streams of municipal effluent treatment plants. Bioresour. Technol. 268, 797–810. https://doi.org/10.1016/j.biortech.2018.07.020.

Ester, M., Kriegel, H.-P., Sander, J., Xu, X., 1996. A density-based algorithm for discovering clusters in large spatial databases with noise. In: Kdd, pp. 226–231.

Fang, F., Ni, B., Li, W., Sheng, G., Yu, H., 2011. A simulation-based integrated approach to optimize the biological nutrient removal process in a full-scale wastewater treatment plant. Chem. Eng. J. 174, 635–643. https://doi.org/10.1016/j.cej.2011.09.079.

Frison, N., Katsou, E., Malamis, S., Oehmen, A., Fatone, F., 2015. Development of a novel process integrating the treatment of sludge reject water and the production of polyhydroxyalkanoates (PHAs). Environ. Sci. Technol. 49, 10877–10885.

Gabarró, J., González-Cárcamo, P., Ruscalleda, M., Ganigué, R., Gich, F., Balaguer, M.D., Colprim, J., 2014. Anoxic phases are the main N2O contributor in partial nitritation reactors treating high nitrogen loads with alternate aeration. Bioresour. Technol. 163, 92–99. https://doi.org/10.1016/j.biortech.2014.04.019.

Haimi, H., Mulas, M., Corona, F., Vahala, R., 2013. Data-derived soft-sensors for biological wastewater treatment plants: an overview. Environ. Model. Software 47, 88–107. https://doi.org/10.1016/j.envsoft.2013.05.009.

IPCC, 2013. The Physical Science Basis. Contribution of Working Group I to the Fifth Assessment Report of the Intergovernmental Panel on Climate Change. Cambridge University Press, USA.

Itokawa, H., Hanaki, K., Matsuo, T., 2001. Nitrous oxide production in high-loading biological nitrogen removal process under low cod/n ratio condition. Water Res. 35, 657–664. https://doi.org/10.1016/S0043-1354(00)00309-2.

Janus, H.M., van der Roest, H.F., 1997. Don't reject the idea of treating reject water. Water Sci. Technol. 35, 27–34. https://doi.org/10.2166/wst.1997.0351.

Jaramillo, F., Orchard, M., Muñoz, C., Antileo, C., Sáez, D., Espinoza, P., 2018. On-line estimation of the aerobic phase length for partial nitrification processes in SBR based on features extraction and SVM classification. Chem. Eng. J. 331, 114–123. https://doi.org/10.1016/j.cej.2017.07.185.

Kampschreur, M.J., Poldermans, R., Kleerebezem, R., van der Star, W.R.L., Haarhuis, R., Abma, W.R., Jetten, M.S.M., van Loosdrecht, M.C.M., 2009. Emission of nitrous oxide and nitric oxide from a full-scale single-stage nitritation-anammox reactor. Water Sci. Technol. 60, 3211–3217. https://doi.org/10.2166/wst.2009.608.

Kampschreur, M.J., van der Star, W.R.L., Wielders, H.A., Mulder, J.W., Jetten, M.S.M., van Loosdrecht, M.C.M., 2008. Dynamics of nitric oxide and nitrous oxide emission during full-scale reject water treatment. Water Res. 42, 812–826. https://doi.org/10.1016/j.watres.2007.08.022.

Karatzoglou, A., Smola, A., Hornik, K., Zeileis, A., 2004. Kernlab - an S4 package for kernel methods in R. J. Stat. Software 11, 1–20.

Kuhn, M., 2008. Building Predictive Models in R Using the caret Package. Journal of Statistical Software 28. https://doi.org/10.18637/jss.v028.i05.

Lackner, S., Gilbert, E.M., Vlaeminck, S.E., Joss, A., Horn, H., van Loosdrecht, M.C., 2014. Full-scale partial nitritation/anammox experiences–an application survey. Water Res. 55, 292–303.

Law, Y., Lant, P., Yuan, Z., 2013. The confounding effect of nitrite on N2O production by an enriched ammonia-oxidizing culture. Environ. Sci. Technol. 47, 7186–7194. https://doi.org/10.1021/es4009689.

Law, Y., Lant, P., Yuan, Z., 2011. The effect of pH on N 2 O production under aerobic conditions in a partial nitritation system. Water Res. 45, 5934–5944.

Law, Y., Ye, L., Pan, Y., Yuan, Z., 2012. Nitrous oxide emissions from wastewater treatment processes. Philos. Trans. R. Soc. B Biol. Sci. 367, 1265–1277. https://doi.org/10.1098/rstb.2011.0317.

Li, C., Wang, T., Zheng, N., Zhang, J., Ngo, H.H., Guo, W., Liang, S., 2013a. Influence of organic shock loads on the production of N2O in denitrifying phosphorus removal process. Bioresour. Technol. 141, 160–166. https://doi.org/10.1016/j.biortech.2013.03.117. Challenges in Environmental Science and Engineering (CESE-2012).

Li, C., Zhang, J., Liang, S., Ngo, H.H., Guo, W., Zhang, Y., Zou, Y., 2013b. Nitrous oxide generation in denitrifying phosphorus removal process: main causes and control measures. Environ. Sci. Pollut. Res. 20, 5353–5360. https://doi.org/10.1007/s11356-013-1530-3.

Liu, Y.-J., Gu, J., Liu, Y., 2018. Energy self-sufficient biological municipal wastewater reclamation: present status, challenges and solutions forward. Bioresour. Technol. 269, 513–519. https://doi.org/10.1016/j.biortech.2018.08.104.

Longo, S., d'Antoni, B.M., Bongards, M., Chaparro, A., Cronrath, A., Fatone, F., Lema, J.M., Mauricio-Iglesias, M., Soares, A., Hospido, A., 2016. Monitoring and diagnosis of energy consumption in wastewater treatment plants. A state of the art and proposals for improvement. Appl. Energy 179, 1251–1268. https://doi.org/10.1016/j.apenergy.2016.07.043.

Luts, J., Ojeda, F., Van de Plas, R., De Moor, B., Van Huffel, S., Suykens, J.A.K., 2010. A tutorial on support vector machine-based methods for classification problems in chemometrics. Anal. Chim. Acta 665, 129–145. https://doi.org/10.1016/j.aca.2010.03.030.

Massara, T.M., Malamis, S., Guisasola, A., Baeza, J.A., Noutsopoulos, C., Katsou, E., 2017. A review on nitrous oxide (N 2 O) emissions during biological nutrient removal from municipal wastewater and sludge reject water. Sci. Total Environ. 596, 106–123.

Newhart, K.B., Holloway, R.W., Hering, A.S., Cath, T.Y., 2019. Data-driven performance analyses of wastewater treatment plants: a review. Water Res. 157, 498–513. https://doi.org/10.1016/j.watres.2019.03.030.

Pan, Y., Ni, B.-J., Bond, P.L., Ye, L., Yuan, Z., 2013. Electron competition among nitrogen oxides reduction during methanol-utilizing denitrification in wastewater treatment. Water Res. 47, 3273–3281. https://doi.org/10.1016/j.watres.2013.02.054.

Peng, L., Carvajal-Arroyo, J.M., Seuntjens, D., Prat, D., Colica, G., Pintucci, C., Vlaeminck, S.E., 2017. Smart operation of nitritation/denitritation virtually abolishes nitrous oxide emission during treatment of co-digested pig slurry centrate. Water Res. 127, 1–10. https://doi.org/10.1016/j.watres.2017.09.049.

Peng, L., Ni, B.-J., Ye, L., Yuan, Z., 2015. The combined effect of dissolved oxygen and nitrite on N 2 O production by ammonia oxidizing bacteria in an enriched nitrifying sludge. Water Res. 73, 29–36.

Pijuan, M., Torà, J., Rodríguez-Caballero, A., César, E., Carrera, J., Pérez, J., 2014. Effect of process parameters and operational mode on nitrous oxide emissions from a nitritation reactor treating reject wastewater. Water Res. 49, 23–33. https://doi.org/10.1016/j.watres.2013.11.009.

Raghavendra, N.S., Deka, P.C., 2014. Support vector machine applications in the field of hydrology: a review. Appl. Soft Comput. 19, 372–386. https://doi.org/10.1016/j.asoc.2014.02.002.

Ren, Y., Ngo, H.H., Guo, W., Ni, B.-J., Liu, Y., 2019. Linking the nitrous oxide production and mitigation with the microbial community in wastewater treatment: a review. Bioresour. Technol. Rep. 7, 100191. https://doi.org/10.1016/j.biteb.2019.100191.

Ribera-Guardia, A., Marques, R., Arangio, C., Carvalheira, M., Oehmen, A., Pijuan, M., 2016. Distinctive denitrifying capabilities lead to differences in N2O production by denitrifying polyphosphate accumulating organisms and denitrifying glycogen accumulating organisms. Bioresour. Technol. 219, 106–113. https://doi.org/10.1016/j.biortech.2016.07.092.

Rodriguez-Caballero, A., Aymerich, I., Marques, R., Poch, M., Pijuan, M., 2015. Minimizing N2O emissions and carbon footprint on a full-scale activated sludge sequencing batch reactor. Water Res. 71, 1–10. https://doi.org/10.1016/j.watres.2014.12.032.

Rodriguez-Garcia, G., Frison, N., Vázquez-Padín, J.R., Hospido, A., Garrido, J.M., Fatone, F., Bolzonella, D., Moreira, M.T., Feijoo, G., 2014. Life cycle assessment of nutrient removal technologies for the treatment of anaerobic digestion supernatant and its integration in a wastewater treatment plant. Sci. Total Environ. 490, 871–879. https://doi.org/10.1016/j.scitotenv.2014.05.077.

Sarni, W., White, C., Webb, R., Cross, K., Glotzbach, R., 2019. Industry Leaders Chart the Transformation Journey. International Water Association (IWA) and Xylem White Paper.

Schaubroeck, T., De Clippeleir, H., Weissenbacher, N., Dewulf, J., Boeckx, P., Vlaeminck, S.E., Wett, B., 2015. Environmental sustainability of an energy self-sufficient sewage treatment plant: improvements through DEMON and co-digestion. Water Res. 74, 166–179. https://doi.org/10.1016/j.watres.2015.02.013.

Schulthess, R.v., Kühni, M., Gujer, W., 1995. Release of nitric and nitrous oxides from denitrifying activated sludge. Water Res. 29, 215–226. https://doi.org/10.1016/0043-1354(94)E0108-I.

Seshan, H., Goyal, M.K., Falk, M.W., Wuertz, S., 2014. Support vector regression model of wastewater bioreactor performance using microbial community

diversity indices: effect of stress and bioaugmentation. Water Res. 53, 282–296. https://doi.org/10.1016/j.watres.2014.01.015.
Shi, S., Xu, G., 2018. Novel performance prediction model of a biofilm system treating domestic wastewater based on stacked denoising auto-encoders deep learning network. Chem. Eng. J. 347, 280–290. https://doi.org/10.1016/j.cej.2018.04.087.
Stenström, F., Tjus, K., Jansen, J. la C., 2014. Oxygen-induced dynamics of nitrous oxide in water and off-gas during the treatment of digester supernatant. Water Sci. Technol. 69, 84–91. https://doi.org/10.2166/wst.2013.558.
Su, Q., Domingo-Félez, C., Zhang, Z., Blum, J.-M., Jensen, M.M., Smets, B.F., 2019. The effect of pH on N2O production in intermittently-fed nitritation reactors. Water Res. 156, 223–231. https://doi.org/10.1016/j.watres.2019.03.015.
Tallec, G., Garnier, J., Billen, G., Gousailles, M., 2006. Nitrous oxide emissions from secondary activated sludge in nitrifying conditions of urban wastewater treatment plants: effect of oxygenation level. Water Res. 40, 2972–2980. https://doi.org/10.1016/j.watres.2006.05.037.
van Loosdrecht, M.C.M., Salem, S., 2006. Biological treatment of sludge digester liquids. Water Sci. Technol. J. Int. Assoc. Water Pollut. Res. 53, 11–20.
Vasilaki, V., Massara, T.M., Stanchev, P., Fatone, F., Katsou, E., 2019. A decade of nitrous oxide (N2O) monitoring in full-scale wastewater treatment processes: a critical review. Water Res. 161, 392–412. https://doi.org/10.1016/j.watres.2019.04.022.
Vasilaki, V., Volcke, E.I.P., Nandi, A.K., van Loosdrecht, M.C.M., Katsou, E., 2018. Relating N2O emissions during biological nitrogen removal with operating conditions using multivariate statistical techniques. Water Res. 140, 387–402. https://doi.org/10.1016/j.watres.2018.04.052.
Wan, X., Baeten, J.E., Volcke, E.I.P., 2019. Effect of operating conditions on N2O emissions from one-stage partial nitritation-anammox reactors. Biochem. Eng. J. 143, 24–33. https://doi.org/10.1016/j.bej.2018.12.004.
Wang, Y., Geng, J., Ren, Z., He, W., Xing, M., Wu, M., Chen, S., 2011. Effect of anaerobic reaction time on denitrifying phosphorus removal and N2O production. Bioresour. Technol. 102, 5674–5684. https://doi.org/10.1016/j.biortech.2011.02.080.
Wang, Z., Meng, Y., Fan, T., Du, Y., Tang, J., Fan, S., 2015. Phosphorus removal and N2O production in anaerobic/anoxic denitrifying phosphorus removal process: long-term impact of influent phosphorus concentration. Bioresour. Technol. 179, 585–594. https://doi.org/10.1016/j.biortech.2014.12.016.
Zhou, X., Zhang, X., Zhang, Z., Liu, Y., 2018. Full nitration-denitration versus partial nitration-denitration-anammox for treating high-strength ammonium-rich organic wastewater. Bioresour. Technol. 261, 379–384. https://doi.org/10.1016/j.biortech.2018.04.049.
Zhou, Y., Pijuan, M., Zeng, R.J., Yuan, Z., 2008. Free nitrous acid inhibition on nitrous oxide reduction by a denitrifying-enhanced biological phosphorus removal sludge. Environ. Sci. Technol. 42, 8260–8265. https://doi.org/10.1021/es800650j.
Zhu, X., Chen, Y., 2011. Reduction of N2O and NO generation in Anaerobic–Aerobic (low dissolved oxygen) biological wastewater treatment process by using sludge alkaline fermentation liquid. Environ. Sci. Technol. 45, 2137–2143. https://doi.org/10.1021/es102900h.